

NO-A167 647

OPTIMIZATION OF THE THERMOELECTRIC FIGURE OF MERIT OF
FINE-GRAINED SEMICO. (U) UNIVERSITY OF WALES INST OF
SCIENCE AND TECHNOLOGY CARDIFF* D N ROME FEB 86

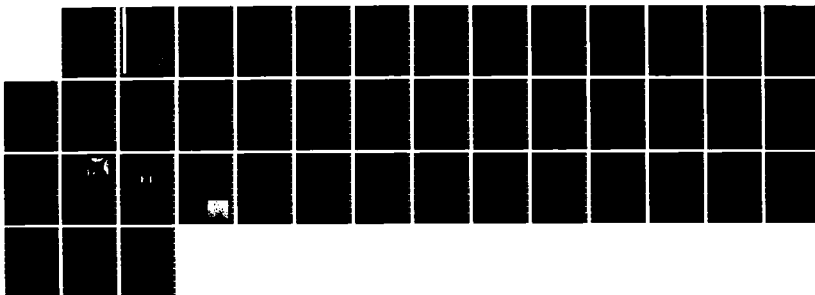
1/1

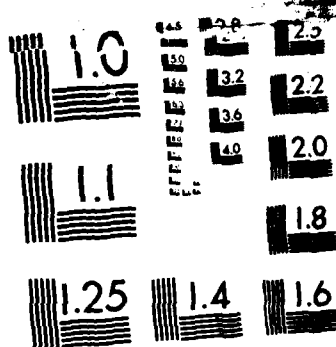
UNCLASSIFIED

DAJA45-84-C-0029

F/G 20/12

NL





MICROCOPY RESOLUTION TEST CHART
NATIONAL BUREAU OF STANDARDS-1963-A

AD-A167 647

R+D-4049A-EE

10

OPTIMIZATION OF THE THERMOELECTRIC FIGURE OF MERIT
OF FINE-GRAINED SEMICONDUCTOR MATERIALS
BASED UPON LEAD TELLURIDE

Final Technical Report

by

D M ROWE
February 1986

United States Army
EUROPEAN RESEARCH OFFICE OF THE U.S. ARMY
London England
Contract Number DAJA45-84-C-0029
UNIVERSITY OF WALES INSTITUTE OF SCIENCE AND TECHNOLOGY

Approved for Public Release Distribution unlimited

DTIC
ELECTE
S MAY 5 1986 D
A

86 5 2 013

unclassified

SECURITY CLASSIFICATION OF THIS PAGE (When Data Entered)

REPORT DOCUMENTATION PAGE		READ INSTRUCTIONS BEFORE COMPLETING FORM
1. REPORT NUMBER	2. GOVT ACCESSION NO.	3. RECIPIENT'S CATALOG NUMBER
AD-A167647		
4. TITLE (and Subtitle) OPTIMIZATION OF THE THERMOELECTRIC FIGURE OF MERIT OF FINE-GRAINED SEMICONDUCTOR MATERIALS BASED UPON LEAD TELLURIDE.		5. TYPE OF REPORT & PERIOD COVERED Final Technical 31 August 1984-30 March 1986
		6. PERFORMING ORG. REPORT NUMBER
7. AUTHOR(s) D.M. ROWE		8. CONTRACT OR GRANT NUMBER(s) DAJA45-84-C-0029
9. PERFORMING ORGANIZATION NAME AND ADDRESS UNIVERSITY OF WALES INSTITUTE OF SCIENCE AND TECHNOLOGY P.O. BOX 25, BUTE BUILDING, KING EDWARD VII AVE. CARDIFF, CFI 3XE		10. PROGRAM ELEMENT, PROJECT, TASK AREA & WORK UNIT NUMBERS 61102A-1T161102BH57
11. CONTROLLING OFFICE NAME AND ADDRESS U.S. ARMY RESEARCH DEVELOPMENT AND STANDARDIZATION GP-UK FPO BOX 65, NY 09510-1500		12. REPORT DATE
		13. NUMBER OF PAGES
14. MONITORING AGENCY NAME & ADDRESS (if different from Controlling Office) U.S. ARMY RESEARCH OFFICE PO BOX 12211 RESEARCH TRIANGLE PARK, NC 27709		15. SECURITY CLASS. (of this report) UNCLASSIFIED
		15a. DECLASSIFICATION DOWNGRADING SCHEDULE
16. DISTRIBUTION STATEMENT (of this Report) APPROVED FOR PUBLIC RELEASE: DISTRIBUTION UNLIMITED.		
17. DISTRIBUTION STATEMENT (of the abstract entered in Block 20, if different from Report)		
18. SUPPLEMENTARY NOTES		
19. KEY WORDS (Continue on reverse side if necessary and identify by block number) THERMOELECTRICS, LEAD TELLURIDE MATERIALS, THERMAL DIFFUSIVITY, PHONONGRAIN BOUNDARY SCATTERING, FINE GRAINED COMPACTS.		
20. ABSTRACT (Continue on reverse side if necessary and identify by block number) Lead telluride type semiconductors are used in the fabrication of thermoelectric modules currently employed in a number of U.S. military applications. This report covers the programme of research undertaken in the Department of Physics, Electronics and Electrical Engineering at UWIST Cardiff to produce materials based upon lead telluride with improved "figures of merit" and hence greater thermoelectric conversion efficiency. One way of improving the figure of merit is by reducing the lattice thermal		

20. continued..

conductivity of the material. This can be achieved by increasing phonon-grain boundary scattering. A realistic theoretical model has been developed for lead telluride and used to investigate the lattice thermal conductivity as a function of grain size and level of doping. In optimally doped material (10^{24} to 10^{25} cm⁻³) with a grain size of $1\mu\text{m}$ the reduction in lattice thermal conductivity was predicted to be 4-6 percent compared with equivalent single crystal. Thermal diffusivity measurements on small grained compacts supported this prediction.

Phonon grain boundary scattering is enhanced in semiconductor alloys because of the presence of disorder scattering and the theoretical model was extended to take this factor into account. PbSnTe and PbGeTe were identified as alloys whose lattice thermal conductivity could be significantly decreased by a reduction in grain size and in optimally doped compacted material with a grain size of $0.5\mu\text{m}$ the reduction compared to equivalent single crystal material was estimated to be 11 and 14 percent respectively.

It is concluded that provided the electrical properties of compacted lead telluride material can be maintained close to that of single crystal; the thermoelectric figure of merit can be substantially improved by employing a fine grain size. In PbGeTe with a grain size of $1\mu\text{m}$, the improvement in the thermoelectric figure of merit is estimated to be about 10 percent.

OPTIMIZATION OF THE THERMOELECTRIC FIGURE OF MERIT
OF FINE-GRAINED SEMICONDUCTOR MATERIALS
BASED UPON LEAD TELLURIDE

Abstract

Lead telluride type semiconductors are used in the fabrication of thermoelectric modules currently employed in a number of US military applications. This report covers the programme of research undertaken in the Department of Physics, Electronics and Electrical Engineering at UWIST Cardiff to produce materials based upon lead telluride with improved "figures of merit" and hence greater thermoelectric conversion efficiency.

One way of improving the figure of merit is by reducing the lattice thermal conductivity of the material. This can be achieved by increasing phonon-grain boundary scattering. A realistic theoretical model has been developed for lead telluride and used to investigate the lattice thermal conductivity as a function of grain size and level of doping. In optimally doped material (10^{24} - 10^{25}m^{-3}) with a grain size of $1\mu\text{m}$, the reduction in lattice thermal conductivity was predicted to be 4-6 percent compared with equivalent single crystal. Thermal diffusivity measurements on small grained compacts supported this prediction.

Phonon grain boundary scattering is enhanced in semiconductor alloys because of the presence of disorder scattering and the theoretical model was extended to take this factor into account. PbSnTe and PbGeTe were identified as alloys whose lattice thermal conductivity could be significantly decreased by a reduction in grain size and in optimally doped compacted material with a grain size of $0.5\mu\text{m}$ the reduction compared to equivalent single crystal material was estimated to be 11 and 14 percent respectively.

It is concluded that provided the electrical properties of compacted lead telluride material can be maintained close to that of single crystal; the thermoelectric figure of merit can be substantially improved by employing a fine grain size. In PbGeTe with a grain size of $1\mu\text{m}$, the improvement in the thermoelectric figure of merit is estimated to be about 10 percent.

THERMOELECTRICS, LEAD TELLURIDE MATERIALS, THERMAL DIFFUSIVITY, PHONON-GRAIN BOUNDARY SCATTERING, FINE GRAINED COMPACTS.

Contents

- I List of Figures.
- II General Introduction
- III Objectives
- IV Development of a theoretical model for lead telluride.
 - 1. Introduction
 - 2. Lattice thermal conductivity
 - 3. Electronic contribution to the thermal conductivity.
 - (i) Introduction
 - (ii) Carrier scattering by acoustic phonons
 - (iii) Carrier scattering by optical phonons
 - (iv) Multivalley energy band structure and intervalley scattering.
 - 4. Thermoelectric figure of merit
- V Theoretical Analysis
 - 1. Lead telluride
 - (i) Relative reductions in the lattice thermal conductivity
 - (ii) The ratio λ_e/λ_L and the Lorenz factor
 - (iii) Electronic thermal conductivity
 - (iv) Total thermal conductivity
 - 2. Disordered lead telluride
 - (i) Introduction
 - (ii) Reduction in the lattice thermal conductivity
 - 3. Alloys based upon lead telluride (PbSnTe, PbGeTe)
 - (i) Introduction
 - (ii) Reduction in the lattice thermal conductivity
 - (iii) Effect of small grain size on the thermoelectric figure of merit
- VI Experimental programme of work
 - 1. Introduction
 - 2. Charge material preparation
 - (i) $<5\mu\text{m}$ grain size material
 - (ii) $<0.5\mu\text{m}$ grain size material
 - 3. Hot press
 - 4. Pressing procedure
 - 5. Physical properties of compacts.
 - 6. Transport properties.
 - (i) Introduction
 - (ii) Seebeck and electrical resistivity measurements
 - (iii) Thermal diffusivity and thermal conductivity measurements.
- VII Discussion and conclusions
- VIII Acknowledgments
- IX References



Accession For		NTIS GRA&I		<input checked="" type="checkbox"/>	<input type="checkbox"/>	<input type="checkbox"/>
		DTIC TAB				
		Unannounced				
		Justification				
By		Distribution/				
Availability Codes						
Avail and/or						
Dist Special						
				A1		

I LIST OF FIGURES

- Figure 1. Plot of $\lambda_L(\text{sintered})/\lambda_L(\text{single crystal})$ for unalloyed lead telluride at 300K as a function of grain size and level of doping.
- Figure 2. The ratio λ_e/λ_L and the Lorenz factor " r " as a function of reduced Fermi energy (ξ) for lead telluride at 300K.
- Figure 3. The ratio λ_e/λ_L as a function of reduced Fermi energy (ξ) at different temperatures.
- Figure 4. The Lorenz factor r as a function of temperature at different carrier concentrations.
- Figure 5. The electronic thermal conductivity (acoustic scattering) of lead telluride as a function of carrier concentration and temperature.
- Figure 6. The electronic thermal conductivity (polar optical scattering) of lead telluride as a function of carrier concentration and temperature.
- Figure 7. The total thermal conductivity (acoustic scattering) of lead telluride as a function of carrier concentration and temperature.
- Figure 8. The total thermal conductivity (acoustic and polar optical scattering) of lead telluride as a function of temperature.
- Figure 9. The total thermal conductivity of lead telluride versus carrier concentration for "single crystal" and $1\mu\text{m}$ grain size material.
- Figure 10. The ratio $\lambda_L(\text{sintered})/\lambda_L(\text{single crystal})$ at room temperature for highly disordered alloys as a function of grain size and level of doping.
- Figure 11. Effect of small grain size on the thermoelectric figure of merit of highly disordered alloys of lead telluride.
- Figure 12. Reduction in the lattice thermal conductivity of PbTe-SnTe at 300K with decrease in grain size.
- Figure 13. Reduction in the lattice thermal conductivity of PbGe-GeTe at 300K with decrease in grain size.
- Figure 14. Photomicrograph of $<0.5\mu\text{m}$ lead telluride powder.
- Figure 15. Hot Press arrangement.
- Figure 16. Dependence of density of PbTe compacts on compacting pressure.
- Figure 17. Photomicrograph of $<0.5\mu\text{m}$ grain size compacted lead telluride.
- Figure 18. Reduction in thermal conductivity of PbTe with decrease in grain size (L).

Table 1. Important material parameters for lead telluride.

Table 2. λ_e/λ_L for lead telluride corresponding to ξ_{opt} . (non-parabolic bands, acoustic phonon scattering).

Table 3. λ_e/λ_L for lead telluride corresponding to ξ_{opt} . (optical phonon, acoustic phonon and combined).

II GENERAL INTRODUCTION

Multifuel thermoelectric generators employing modules based upon lead telluride technology are used in a number of military applications¹. In addition to their multifuel capability these generators are difficult to detect by visual, aural, or thermal infrared.² Clearly any improvement in the thermoelectric conversion efficiency of the generator would result in a saving in fuel - an important consideration when the device is used in a tactical situation.

The factors which determine the conversion efficiency (η) of a thermoelectric generator have been exhaustively dealt with in the literature.³⁻¹¹ It is suffice to state that once the operating temperature and the temperature difference over which the generator operates has been decided, η depends solely upon the so called figure of merit Z of the thermocouple material, where $Z = \alpha^2 \sigma / \lambda$, α is the Seebeck coefficient, σ the electrical conductivity. The thermal conductivity λ is the sum of λ_L , a contribution due to the lattice and λ_e an electron (or hole) contribution.

The parameters which occur in the expression for the figure of merit are functions of the carrier concentration (usually expressed in terms of the reduced Fermi energy ξ) and in the established high temperature thermoelectric material silicon-germanium alloy, Z is optimized at around 10^{25} - 10^{26} m^{-3} .¹² However, at these high carrier concentrations λ_L still accounts for about 75 percent of λ and it is anticipated that λ_L will contribute a similar proportion to the thermal conductivity of lead telluride. Consequently a reduction in λ_L would result in a corresponding increase in the figure of merit of lead telluride and hence in the materials thermoelectric conversion efficiency.

It has been reported that phonon-grain boundary scattering has a significant effect on reducing the lattice thermal conductivity of silicon germanium alloys.¹³⁻¹⁵ This phenomenon does not appear to be accompanied by a deterioration in the other parameters which occur in the figure of merit although the long term behaviour of small grain size material when subjected to high temperatures has not been reported. Consequently small grain size silicon germanium alloys exhibit a higher figure of merit than comparable "single crystal" or large grain size material. Grain boundary scattering is particularly favoured in silicon-germanium alloy because the large difference in atomic masses of the constituent atoms give rise to substantial alloy disorder scattering. However, this

phenomenon will also be present in other thermoelectric alloys and in alloy compounds such as those based upon lead telluride.

The United States Army is currently evaluating the performance of a number of improved thermoelectric materials for possible use in future thermoelectric generators. Evidently information on the reduction in thermal conductivity and hence potential improvement in thermoelectric performance, which accompanies the use of small grain size lead telluride type material and on the conditions which optimise the thermoelectric figure of merit of these materials is relevant to their programme of material evaluation.

III OBJECTIVES

The objectives of the programme of research described in this report were:-

- 1(a) Initially to develop a semiquantitative theoretical model of lead telluride. Use the model to estimate the *relative reduction* in the lattice thermal conductivity compared to single crystal material with decrease in grain size and hence improvement in the thermoelectric figure of merit.
- (b) Substantiate the theoretical prediction by preparing $<5\mu\text{m}$ grain size compacts of lead telluride and measuring the relevant transport properties.
- 2 Depending upon the success or otherwise in achieving these initial objectives the second phase of the work was to:-
 - (a) Develop a realistic theoretical model for the *absolute magnitude* of the thermal conductivity of lead telluride. Use the model to identify alloys based on lead telluride whose lattice thermal conductivity offer the best potential for reduction as a result of phonon-grain boundary scattering. Determine the conditions for optimising the thermoelectric figure of merit of these alloys.
 - (b) Attempt to comminute very small grain size ($<0.5\mu\text{m}$) lead telluride material.

For convenience in presentation the work reported is divided into two stages 1. Theoretical and 2. Experimental

IV DEVELOPMENT OF A THEORETICAL MODEL FOR LEAD TELLURIDE

1. Introduction

The initial objective to estimate the relative reduction in lattice thermal conductivity, compared to single crystal, with decrease in grain size was fairly straightforward. A two band model with parabolic multivalled energy band structure was considered. Acoustic phonon

scattering was taken to be the dominant scattering mechanism, intervalley scattering is neglected and no distinction made between the conductivity effective mass and the density-of-states effective mass. Although the model was later improved, preliminary calculations indicated that the *relative changes* in thermal conductivity due to phonon-grain boundary scattering, and consequent relative changes in the thermoelectric figure of merit are fairly insensitive to the inclusion of these refinements.

However, the development of a realistic model for lead telluride for use in identifying potentially good alloys based on lead telluride presented considerable difficulties. The theoretical model must give good agreement with experimental data cited in the literature and this involved obtaining the separate electronic (λ_e) and lattice (λ_L) contributions to the thermal conductivity. A prerequisite for this analysis is a knowledge of the Lorenz number. A literature survey revealed that there is very little European or United States published information on the value and behaviour of the Lorenz number for lead telluride. The realistic model developed considers both acoustic and optical phonon scattering. It takes into account the non parabolic nature and multivalled structure of the energy bands, including intervalley scattering. Minority carrier effects will also be significant over part of the temperature range of operation of the materials and should be included. The principal elements of the theoretical model are discussed in the following section.

2. Lattice thermal conductivity

At temperatures above room temperature, a simple formulation for the lattice thermal conductivity can be used which includes the various phonon scattering mechanisms^{16,17}. The lattice thermal conductivity is expressed in terms of three parameters A, B and C which relate to phonon scattering by alloy disorder, free carriers and grain boundaries respectively. Defining λ_0 as the thermal conductivity of a large, perfect (notional) crystal, the lattice thermal conductivity is given by:-

$$\frac{\lambda_L}{\lambda_0} = \left[1 + \frac{5k_0}{9} \right]^{-1} \left[L_2(A, B, C) + \frac{\left(\frac{k_0}{1+k_0} \right) L_4^2(A, B, C)}{\left\{ \frac{1}{5} - \left(\frac{k_0}{1+k_0} \right) L_6(A, B, C) \right\}} \right]$$

$$\text{where } L_n(A, B, C) = \int_0^1 \frac{x^n dx}{Ax^4 + x^2 + Bx + C}$$

here $x = \hbar\omega/k_B T$ and $k_0 = \tau_U/\tau_N$ is the ratio of the phonon relaxation times for Umklapp and Normal processes. k_B is Boltzmann's constant and T is the temperature. There is no advantage in this present study to undertake detailed calculations of the contributions to the thermal conductivity from separate polarizations and an average acoustic branch is assumed. The various phonon relaxation times are as described in the literature;^{14, 16, 17} the phonon-electron scattering relaxation time is given by

$$\tau_{pe}^{-1} = B'x$$

A, B and C are given by

$$A = \frac{\pi^2 \Omega_0 \lambda_0 \omega_D}{2 V_S^2 k_B \left(1 + \frac{5k_0}{9}\right)} \quad \begin{array}{l} \text{Alloy disorder} \\ \text{scattering} \end{array}$$

$$B = \frac{2\pi^2 \lambda_0 \hbar B'}{k_B L \omega_D^3 \left(1 + \frac{5k_0}{9}\right)} \quad \begin{array}{l} \text{Free carrier} \\ \text{scattering} \end{array}$$

$$C = \frac{2\pi^2 \lambda_0 \hbar \overset{\text{Grain size } L}{V_S^2}}{k_B L \omega_D^3 \left(1 + \frac{5k_0}{9}\right)} \quad \begin{array}{l} \text{Grain boundary} \\ \text{scattering} \end{array}$$

The various parameters have the same meaning as in the literature^{14, 16, 17}. It is usual to express C in terms of a parameter D, which is inversely proportional to the grain size L and they are related

by $D=CT$ where T is the temperature. $A=0$ corresponds to unalloyed material with no disorder present, $B=0$ corresponds to undoped material and $C=0$ to single crystal material. In general $\lambda(A,B,C=0) = \lambda_{\text{single}}$ represents the lattice thermal conductivity of a doped single crystal alloy while $\lambda(A,B,C) = \lambda_{\text{sintered}}$ represents the lattice thermal conductivity of a compacted (sintered) alloy.

3. Electronic contribution to the thermal conductivity

(i) Introduction

Lead telluride and its alloys possess a narrow energy band gap (E_g). These materials have small electron effective masses and the density of states which varies as $m^{3/2}$ is also relatively small. Consequently a relatively small number of carriers will be sufficient to fill the bands up to high energy levels. The effective mass of electrons near the top of the conduction band become energy dependent¹⁸. In the model adopted a two band conduction band is considered with the following main features; the band extrema for the conduction and valence bands are assumed to be located at the same k value. The energy separation from the other bands at this k value is greater than the main energy gap and the momentum operator has non-zero matrix elements between the states corresponding to the extremal points. Non-parabolicity and the effective mass of both bands are defined by the interaction of the electron and hole bands only. The energy dispersion law is of the form:-

$$\frac{\hbar^2 k_{\perp}^2}{2m_{\perp 0}^*} + \frac{\hbar^2 k_{\parallel}^2}{2m_{\parallel 0}^*} = E \left(1 + \frac{E}{E_g} \right)$$

k_{\perp} and k_{\parallel} are the transverse and longitudinal components of the wave vector and $m_{\perp 0}^*$ and $m_{\parallel 0}^*$ ^{are} ~~and~~ the components of the effective mass tensor near the band extremum. This is usually referred to as the "Kane model". The energy dependence of the effective mass is given by :-

$$m^* = m_0^* \left[1 + \frac{2E}{E_g} \right]$$

For a multivalled structure with N_V equivalent valleys the density of states effective mass is:-

$$m_d^* = N_V^{2/3} (m_{||}^* m_{\perp}^{*2})^{1/3} = N_V^{2/3} m_{d1}^*$$

and the conductivity effective mass:-

$$m_c^{*-1} = \frac{1}{3} (m_{||}^{*-1} + 2m_{\perp}^{*-1})$$

The energy dependence of the effective mass manifests itself in the various transport coefficients; these are expressed in terms of averaged quantities such as $\langle \tau \rangle$, $\langle \tau^2 \rangle$, $\langle \tau(E) \rangle$ etc. In the case of non-parabolic energy bands:-

$$\langle \tau^{n_{Em}} \rangle = \frac{\int_0^\infty (-\partial f / \partial E) [\tau(E) / m^*(E)]^{n_{Em}} dE}{\int_0^\infty (-\partial f / \partial E) (k^3 / m_c^* n) dE}$$

$$\text{where } k = \frac{(2m_{d1}^*)^{1/2} [E(1+E/E_g)]^{1/2}}{\hbar}$$

In lead telluride at room temperature, the contribution of impurity scattering to the carrier mobility is very small and will be negligible at the temperatures of operation of a thermoelectric device. Consequently only electron-phonon scattering mechanisms need to be considered.

3 (ii) Carrier scattering by acoustic phonons

The carrier relaxation time can be written as:-

$$\tau \sim \frac{1}{|M|^2 \rho(\eta)}$$

where $\eta = E/k_B T$ is the reduced carrier energy, M is the matrix element for the electron-phonon interaction and $\rho(\eta)$ is the density of states. The calculation is simplified if it is assumed that the matrix element depends upon energy as for the case of a parabolic band. For scattering by acoustic phonons, this amounts to $|M|^2 = \text{constant}$. The relaxation time is then given by :-

$$\tau_{ac} \sim \frac{1}{\rho(\eta)} \propto \frac{1}{[\eta(1+\beta_g \eta)]^{1/2} (1+2\beta_g \eta)}$$

$$\text{where } \beta_g = k_B T / E_g$$

The appropriate expression for $\tau(\eta)$ which includes the energy dependence of M is given by^{19,20}

$$\tau(\eta)^{-1} = \frac{n k_B T (\rho/N_V)}{\hbar C_1} \epsilon^2 \left[1 - \frac{8\beta_g \eta (1+\beta_g \eta)}{3(1+2\beta_g \eta)^2} \right]$$

where C_1 is the elastic constant related to the average sound velocity, (ρ/N_V) is the density of state in a given valley and ϵ is the deformation potential constant.

The Lorenz factor is given by:-

$$r = \left[\frac{n_{L_{-2}}^1}{n_{L_{-2}}^0} \right] - \delta^2$$

where $\delta = n_{L_{-2}}^1 / n_{L_{-2}}^0$, and $n_{L_i}^m$ are generalised.

Fermi integrals and defined as:-

$$n_{L_i}^m(\xi) = \int_0^\infty \left[- \frac{\partial f}{\partial \eta} \right] \eta^n [n(1+\beta_g \eta)]^m (1+2\beta_g \eta)^i d\eta$$

The reduced electrical conductivity is given by:-

$$\sigma' = k N_V n_{L_{-2}}^0 \frac{T}{(m_C^* \lambda_L)}$$

With the carrier concentration n related to the reduced Fermi energy ξ , by the expression:-

$$n = \frac{(2m_{dO}^* k_B T)^{3/2}}{3\pi^2 \hbar^3} n_{L_O}^{3/2}$$

The carrier mobility μ_{ac} due to acoustic phonon scattering is given by:-

$$\mu_{ac} = \frac{\text{constant}}{m_{CO}^* m_{dO}^{*3/2} T^{3/2}} \frac{n_{L_{-2}}^1}{n_{L_O}^{3/2}}$$

3.(iii) Carrier scattering by polar optical phonons

The carrier relaxation time for scattering by polar optical phonons is given by²⁰

$$\tau_{op}^{-1} = \frac{2^{1/2} e^2 k_B T m_d^{*1/2}}{h^2 (\eta k_B T)^{1/2}} (\epsilon_{\infty}^{-1} - \epsilon_0^{-1}) \frac{1+2\beta_g \eta}{(1+\beta_g \eta)^{1/2}} \\ \times \left[[1 - \epsilon_{\infty} \ln(1 + \epsilon_{\infty}^{-1})] - \frac{2\beta_g \eta (1 + \beta_g \eta)}{(1 + 2\beta_g \eta)^2} [1 + 2\epsilon_{\infty} + 2\epsilon_{\infty}^2 - \ln(1 + \epsilon_{\infty}^{-1})] \right]$$

The Lorenz factor is given by :-

$$x = [L_{-2}^2 / {}^o L_{-2}^2] - \delta^2$$

$$\text{where } \delta = L_{-2}^2 / {}^o L_{-2}^2$$

In the calculations, screening effects have not been taken into account. Polar optical scattering although appreciable in lead telluride materials, is not the dominant scattering mechanism. Consequently neglecting screening effects will not substantially affect the overall electronic transport properties.

The reduced electrical conductivity can be expressed as:-

$$\sigma' = N_V K' T^2 f(\theta_0/T) m_d^* {}^o L_{-2}^2 / (\lambda_L m_C^*)$$

$$\text{with } K' = \frac{4k_B^2}{3e^2 \pi^2 \hbar (\epsilon_{\infty}^{-1} - \epsilon_0^{-1})}$$

where ϵ_0 and ϵ_{∞} are the static dielectric constant and the dielectric constant at high frequencies respectively. θ_0 is the temperature which corresponds to the optical phonon frequency at the zone boundary.

The carrier mobility μ_{op} due to optical phonon scattering is given by:-

$$\mu_{op} = \frac{K'' f(\theta_0/T) {}^o L_{-2}^2}{T^{1/2} m_d^* m_C^* {}^o L_0^{3/2}}$$

$$\text{where } K'' = \frac{8\hbar^2 (2\pi k_B)}{3E (2\pi k_B)^{3/2} (\epsilon_{\infty}^{-1} - \epsilon_0^{-1})}$$

3 (iv) Multivalley energy band structure and intervalley scattering

A multivalley energy band structure together with intervalley scattering must be included in the theoretical model for lead telluride type materials if quantitative correspondence is sought between theory and experimental data. Although the inclusion of a multivalley structure and non-parabolicity of the energy momentum relationship makes the computation lengthy, the model is tractable in the details. The greatest difficulty is in accurately calculating the effect of intervalley scattering. In this analysis a method due to Herring²¹ is followed. The transition of an electron from one valley to another (in k space) is accompanied by a large change in momentum. The phonons which participate in this scattering process lie near the edge of the Brillouin zone. At the Brillouin zone boundary, the acoustic and optical branches are either degenerate or close to one another. The frequency of the intervalley mode ω_i has a value between the frequency of the two modes at the zone boundary, with the relaxation time for intervalley scattering of carriers given by:-

$$\tau_i^{-1} = \frac{W_2 \left\{ \left[(E/k_B\theta_i) + 1 \right]^{1/2} + \exp(\theta_i/T) \operatorname{Re} [C(E/k_B\theta_i) - 1]^{1/2} \right\}}{[\exp(\theta_i/T) - 1]}$$

where W_2 is a rate constant. Averaging τ_i over a Maxwell-Boltzmann distribution function gives for thermal carriers.

$$\langle \tau_i^{-1} \rangle = W_2 (2Z'/\pi)^{1/2} K_1(Z') \sinh(Z')$$

where K_1 is a modified Bessel function of the second kind and $Z' = \theta_i/2T$.

The total relaxation time of carriers is obtained by adding the inverse relaxation times for the acoustic scattering τ_{ac} and intervalley scattering τ_i . The ratio μ/μ_0 , where μ is the mobility can be calculated²¹ as a function of T/θ_i and the mobility obtained for various values of W_2/W_1 ; here $\mu_0 = \mu_{ac}(T/\theta_i)^{3/2}$, $\theta_i = \hbar\omega_i/k_B$ and W_1 is the rate constant for intervalley scattering.

The use of Maxwell-Boltzmann statistics may well be inappropriate at the high carrier concentrations present in thermoelectric semiconductors. However, lead telluride exhibits intervalley scattering to a relatively small degree. Consequently, any shortcomings of the theoretical model which may result from the use of Maxwell-Boltzmann statistics will have little effect on the calculated values of the electronic transport coefficients. The calculation of the Lorenz factor and the ratio λ_e/λ_L

are based upon Fermi-Dirac statistics and are valid at high carrier concentrations.

4. Thermoelectric Figure of Merit

The dimensionless thermoelectric figure of merit ZT for a two band model can be written as²²:-

$$ZT = \frac{(\alpha'_p \sigma'_p - \alpha'_n \sigma'_n)^2}{(\sigma'_n + \sigma'_p)(1 + \alpha'_n Z'_n + \sigma'_p Z'_p) + \sigma'_n \sigma'_p (\delta_n + \delta_p + \xi_g)^2}$$

where α' and σ' are the dimensionless forms of the Seebeck coefficient and electrical conductivity.

V THEORETICAL ANALYSIS

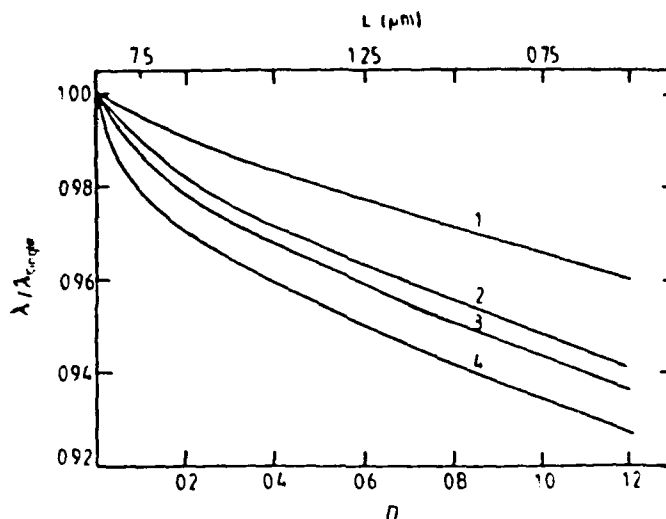
1 Lead Telluride

(i) Relative reduction in thermal conductivity due to phonon-grain boundary scattering.

An estimate can be made of the relative reduction in the lattice thermal conductivity of unalloyed lead telluride with reduction in grain size compared with single crystal material using the model outlined. The results of this calculation are displayed in Figure 1.

Figure 1.

Plot $\lambda_L(\text{sintered})/\lambda_L(\text{single crystal})$ for unalloyed lead telluride at 300K as a function of grain size and level of doping. $k_0 = 1.0$, $A = 0$; curves: 1, $B = 0.050$; 2, $B = 0.010$; 3, $B = 0.005$; 4, $B = 0$.



Although there is some difficulty in making an accurate prediction of the dependence of the lattice thermal conductivity on the various parameters because of a lack of experimental data and the uncertainty in the appropriate value of k_0 it is possible to estimate the range over which the results will vary. In undoped lead telluride the reduction in lattice

thermal conductivity is given by $(1 - \lambda_{L\text{sintered}}/\lambda_{L\text{single crystal}}) \times 100$ for a mean grain size of $1\mu\text{m}$ is around 6 percent. For doped lead telluride (10^{24}m^{-3} – 10^{25}m^{-3}) this reduction is decreased to about 5 percent.

(ii) The ratio λ_e/λ_L and the Lorenz factor \mathcal{L}

Of central importance in a quantitative evaluation of the figure of merit is the contribution to the thermal conductivity which arises from charge carriers. This contribution λ_e/λ_L can conveniently be expressed in terms of the quantity $\sigma'\mathcal{L}$. The calculated values of the ratio λ_e/λ_L and the Lorenz factor are displayed in Figure 2 as a function of the reduced

Figure 2. The ratio λ_e/λ_L and the Lorenz factor \mathcal{L} as a function of reduced Fermi energy (ξ) for lead telluride at 300K. (a) acoustic phonon scattering without intervalley scattering and (b) polar optical scattering. Curves A and B refer to parabolic and non parabolic bands respectively.

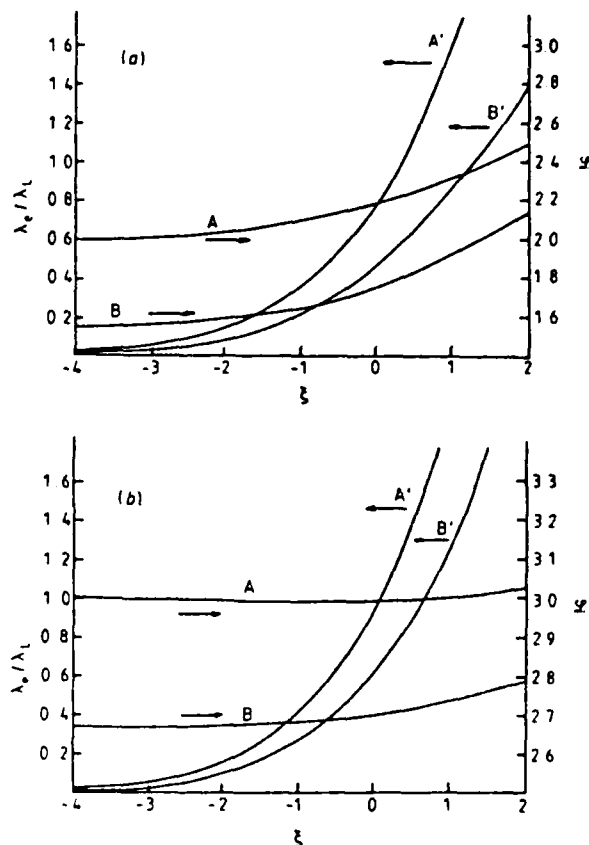
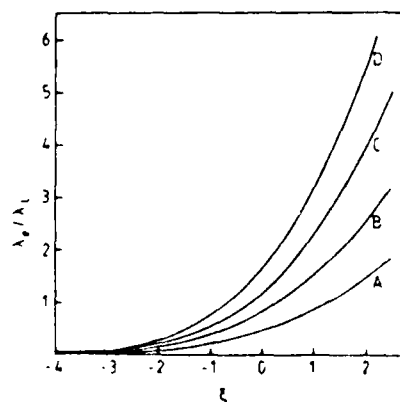


Figure 3. The ratio λ_e/λ_L as a function of reduced Fermi energy (ξ) for lead telluride at different temperatures. A non parabolic energy band is considered with $B_g = k_B T/E_g$; acoustic phonon scattering. Curves (A) 300K (B) 500K (C) 700K (D) 900K.



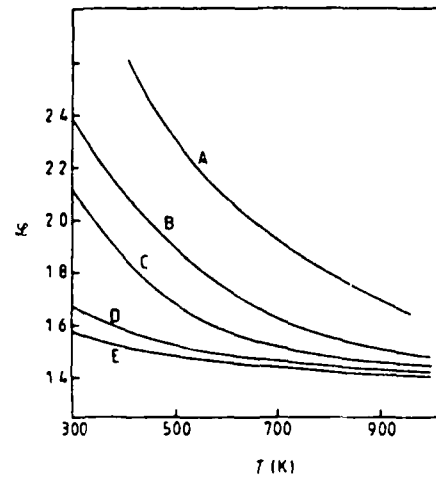
Fermi energy (ξ) for parabolic and non parabolic bands. Scattering of electrons by acoustic and optical modes have been included. Important material parameters for lead telluride are collected in Table 1. In Figure 3 is displayed the ratio λ_e/λ_L versus ξ for lead telluride at different temperatures for a non parabolic energy band. The temperature variation of β_g is obtained from the relationship $\beta_g = k_B T/E_g$. The Lorenz

Table 1. Important Material Parameters for PbTe

C_{11}	ϵ_1	λ_L	N_V	E_g	ϵ_0	ϵ_∞
1.39×10^{11} (Nm ⁻²)	24 (eV)	1.7 (wm ⁻¹ K ⁻¹)	4	0.32 (eV)	400	38

factor is plotted in Figure 4 as a function of temperature for different carrier concentrations.

Figure 4. The Lorenz factor \mathcal{L} for lead telluride as a function of temperature at different carrier concentrations. Acoustic phonon scattering. Curves (A) $3 \times 10^{25} \text{m}^{-3}$, (B) 10^{25}m^{-3} , (C) $5 \times 10^{24} \text{m}^{-3}$, (D) 10^{24}m^{-3} (E) $2 \times 10^{23} \text{m}^{-3}$.



It is apparent from Figure 2 that the ratio λ_e/λ_L corresponding to a particular value of ξ is considerably reduced when the effect of non parabolicity is taken into account. In thermoelectric applications the behaviour of the material in the region of ξ_{opt} (value of the reduced Fermi energy which optimises the thermoelectric figure of merit) is of considerable interest. In Table 2 the ratio λ_e/λ_L for PbTe corresponding to ξ_{opt} at different temperatures is presented for parabolic and non parabolic energy bands. Carrier scattering has been taken to be by acoustic phonons only.

T(k)	ξ_{opt}^\dagger	λ_e/λ_L	λ_e^\ddagger	λ_e/λ_L^\S
		(parabolic band)	(non-parabolic band)	(non parabolic band)
		$\beta_g=0$	$\beta_g=0.08$	$\beta_g=1/\xi_g(T)$
300	-0.75	0.50	0.27	0.25 (0.15)*
500	-0.90	0.70	0.35	0.30
700	-1.20	1.00	0.50	0.40
900	-1.30	1.25	0.65	0.50

\dagger obtained from calculation of the figure of merit and corresponds to about $2 \times 10^{24} \text{ m}^{-3}$.

\ddagger $\beta_g=0.08$ is a realistic estimate of β_g at 300K but because β_g is temperature dependent it becomes less realistic at higher temperatures.

\S $E_g(T) = E_g(300) + 4 \times 10^{-4} (T-300)$; $\xi_g(T) = \frac{E_g(T)}{k_B T} = E_g(T)/k_B T$.

*Includes intervalley scattering $W_2/W_1 = 0.5$.

Table 2. The ratio λ_e/λ_L for lead telluride corresponding to ξ_{opt} at different temperatures and appropriate to parabolic and non-parabolic bands; acoustic phonon scattering.

In Table 3 are collected the room temperature values of λ_e/λ_L at optimum doping appropriate to optical phonon scattering and acoustic phonon scattering, separately and when combined (non-parabolic energy bands).

λ_e/λ_L	λ_e/λ_L	λ_e/λ_L	λ_e/λ_L
(acoustic)	(optical)	(combined)	(observed)
0.25(0.5) †	0.50(0.8) †	0.17	0.15

\dagger obtained using parabolic bands

Table 3. Room temperature values of the ratio λ_e/λ_L at optimum doping (non-parabolic energy bands)

(iii) Electronic Thermal Conductivity

The inclusion of non-parabolicity in the calculation of both scattering mechanism considerably reduces the electronic contribution to the thermal conductivity. The calculated value of the combined scattering is in very good agreement with the experimentally obtained values^{2,3}. Combining the effect of the two scattering mechanisms is not straightforward. A rough estimate can be obtained by assuming ξ at ξ_{opt} to be the same for both cases; the inverse electrical conductivities can

then be added to give the combined values.

In Figure 5 are displayed the calculated values of the electronic thermal conductivity of n-type lead telluride

Figure 5. Electronic thermal conductivity (λ_e) for n-PbTe as a function of carrier concentration and temperature (acoustic scattering and non-parabolic bands). Curves 1,2,3,4 correspond to temperatures of 300, 450, 600, 750K, respectively.

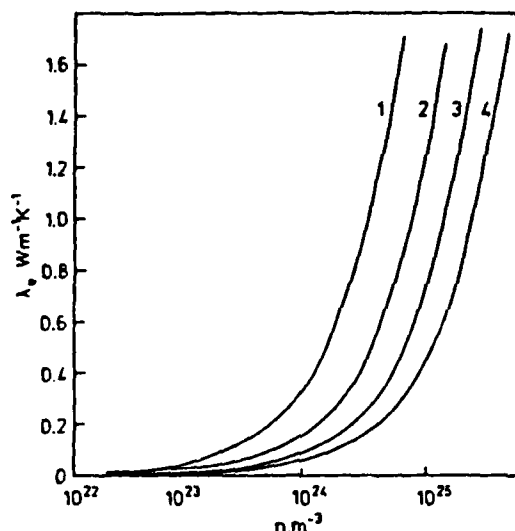
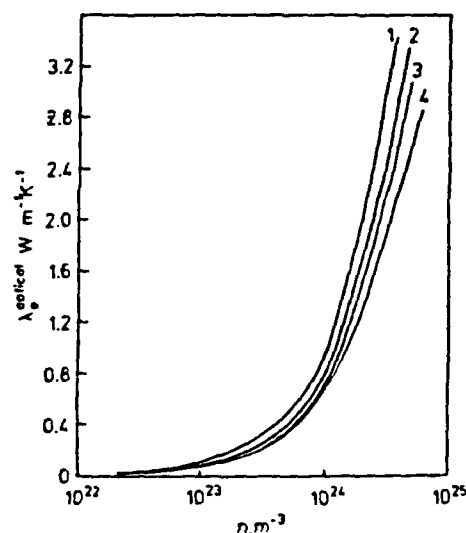


Figure 6. Electronic thermal conductivity ($\lambda_e^{\text{optical}}$) versus carrier concentration. Curves 1,2,3,4 correspond to the temperatures of 300, 450, 600, 750K, respectively.



as a function of carrier concentration at temperatures of 300, 450, 600, and 750K assuming that the electrons are scattered by acoustic phonons. At carrier concentrations 10^{24} m^{-3} the electronic contribution becomes dominant; consequently the contribution due to polar optical scattering (Figure 6) should be included in the calculation of λ_e .

(iv) Total Thermal Conductivity

A reasonable estimate of the temperature variation of the total thermal conductivity can be obtained by assuming a temperature dependence of $1/T$ for the lattice thermal conductivity. The results of this calculation are plotted in Figure 7 assuming acoustic phonon scattering. In Figure 8 the total thermal conductivity is plotted as a function of

temperature for two different carrier concentrations; $n=5 \times 10^{24} \text{ cm}^{-3}$ and 10^{25} cm^{-3} . Curves 1 and 2 correspond to acoustic phonon scattering and include the effect of non-parabolic energy bands. Curves 1' and 2' are the total thermal conductivity with λ_e given by $\lambda_e^{-1} = \lambda_e^{-1} (\text{acoustic}) + \lambda_e^{-1} (\text{optical})$. Evidently the inclusion of polar optical scattering has

Figure 7. Total thermal conductivity $\lambda (= \lambda_L + \lambda_e)$ as a function of carrier concentration and temperature (acoustic scattering). 1,1'-300K; 2,2'-450K; 3,3'-600K; 4,4'-750K. (Dashed lines: parabolic bands; solid lines: non-parabolic bands).

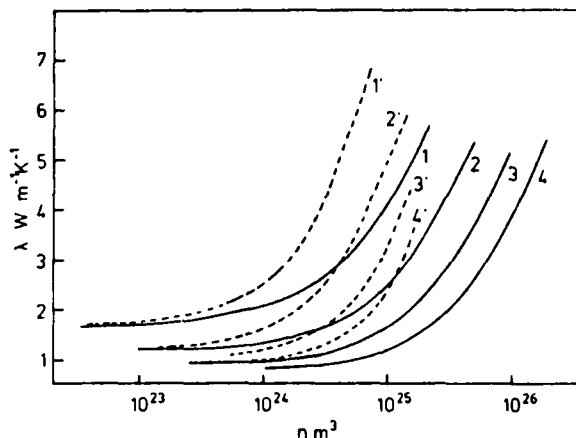
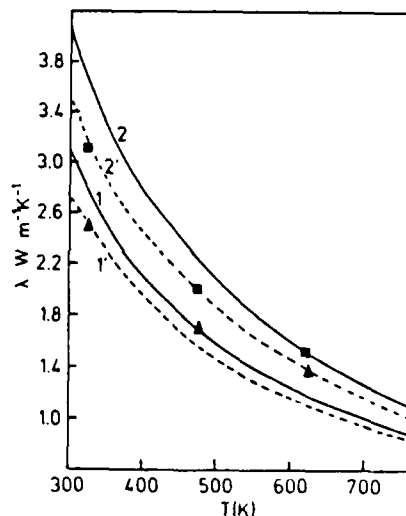


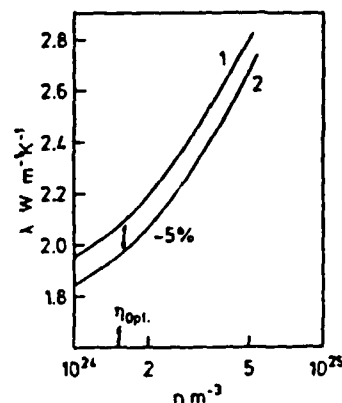
Figure 8. Total thermal conductivity (λ) versus temperature. 1,1'- $5 \times 10^{24} \text{ m}^{-3}$; 2,2'- 10^{25} m^{-3} ; 1',2' include scattering of electrons by polar optical modes along with the acoustic modes. Experimental points by Efimova et al. [13]: $\Delta 5 \times 10^{24} \text{ m}^{-3}$ and $\blacksquare 10^{25} \text{ m}^{-3}$.



an appreciable effect on the total thermal conductivity at carrier concentrations in excess of $5 \times 10^{24} \text{ m}^{-3}$. The calculation of the lattice thermal conductivity in Figure 8 also takes into account the scattering of phonons by free electrons. The parameter B was adjusted to the values of 0.01 and 0.02, curves (1,1') and (2,2') respectively. Excellent agreement is obtained between the calculated values and reported experimental data at around room temperature²⁴. However, it is apparent that the slopes of the theoretical curves are somewhat greater than those based upon experimental data. The inclusion of a photon contribution to the thermal conductivity at higher temperatures is likely to be small for doped samples¹⁹ and is unlikely to account for the differences in slope. In

Figure 9 is displayed the effect of phonon-grain boundary scattering on the room temperature thermal conductivity of small grain size lead telluride. Earlier calculations of this effect²⁵ did not take into account the electronic contribution to the thermal conductivity.

Figure 9. Total thermal conductivity versus carrier concentration for "single crystal" lead telluride and fine-grained material with mean grain size $1\mu\text{m}$.



The calculation assumes an absence of disorder ($A=0$) and consequently the reduction in thermal conductivity corresponds to the situation when boundary scattering is relatively less effective in scattering phonons.¹⁷⁻²⁵ In undoped lead telluride with a mean grain size of $1\mu\text{m}$ the reduction in thermal conductivity will be about 6% whereas in the range of optimum doping encountered in thermoelectric applications ($n \sim 2 \times 10^{24} \text{m}^{-3}$ in lead telluride) this reduces to about 5%.

2. Disordered Lead Telluride

(i) Introduction

As mentioned previously, phonon-grain boundary scattering will be enhanced in alloys. The initial theoretical model, which was developed to obtain an estimate of the relative reduction in the lattice thermal conductivity of lead telluride with decrease in grain size, was extended to include disordered lead telluride (alloys). An estimate was obtained of the dependence of the thermal conductivity and thermoelectric figure of merit on grain size, level of doping for a highly disordered alloy. Preliminary calculations indicated that calculations involving *relative changes* in the thermoelectric figure of merit are fairly insensitive to the inclusion of refinements in the theoretical model. A two band model with a parabolic multivalled structure was considered, acoustic scattering was taken as the dominant scattering mechanism, intervalley scattering was neglected and no distinction made between conductivity effective mass and the density of states effective mass.

(ii) Reduction in the lattice thermal conductivity

Plots of the ratio $\lambda_{\text{sintered}}/\lambda_{\text{single crystal}}$ at room temperature for highly disordered alloys of lead telluride ($A=5$) is displayed in Figure 10 as a function of grain size and level of doping; in material with a mean grain size of about $1\mu\text{m}$ the reduction in lattice thermal conductivity compared to equivalent single crystal material is in the range 11-13 percent.

Figure 10. Plot of $\lambda_{\text{L(sintered)}}/\lambda_{\text{L(single crystal)}}$ for a highly disordered alloy of lead telluride of grain size and level of doping. $k_0 = 1.0, A=5.0$; curves 1, $B=0.050$; 2, $B=0.010$; 3, $B=0.005$; 4, $B=0$

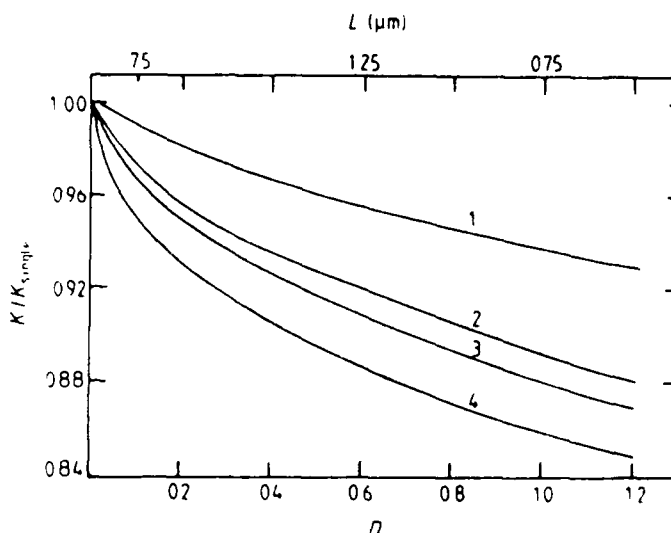
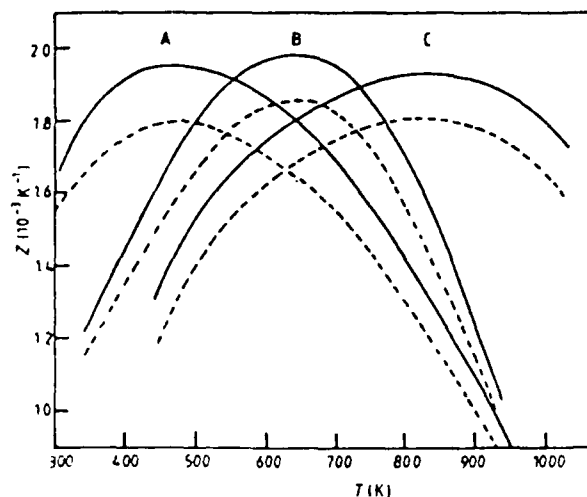


Figure 11. Plots of the thermoelectric figure of merit Z for a highly disordered alloy of lead telluride with three different carrier concentrations n , as a function of temperature: A, $n = 5 \times 10^{24} \text{ m}^{-3}$; B, $n = 10^{25} \text{ m}^{-3}$; C, $n = 2 \times 10^{25} \text{ m}^{-3}$. Curves: — λ_{L} corresponds to material with a mean grain size $\sim 1\mu\text{m}$; - - - λ_{L} corresponds to 'single crystal' or large grain size material



(iii) Effect of small grain size on the thermoelectric figure of merit.

As indicated in Table 2 preliminary calculations of the thermoelectric figure of merit (Z) of unalloyed lead telluride indicated that Z was optimised at room temperature at a reduced Fermi Energy (ϵ) of -0.75 ; which corresponded to a carrier concentration of about $2 \times 10^{24} \text{ m}^{-3}$. The thermoelectric figure of merit for a highly disordered alloy of lead telluride at their different carrier concentrations around optimum doping

is shown in Figure 11 as a function of temperature. The temperature dependence of the effective mass m^* and the energy gap E_g is taken into account using the relationship

$$\frac{1}{m^*} \frac{dm^*}{dT} = \frac{1}{E_g} \frac{dE_g}{dT}$$

$$E_g(T) = E_g(T_0) - \frac{dE_g}{dT} (T-300)$$

with $T_0 = 300K$, $dE_g/dT = 4 \times 10^{-4}$, $m^* = 0.2m_0$ at 300K, λ_L at 300K is $1.70 \text{ Wm}^{-1}\text{K}^{-1}$ and is assumed to vary inversely with temperature. The variation of carrier concentration n with temperature is obtained by relating the variation of Seebeck coefficient with reduced Fermi potential²⁶ to the temperature dependence of the Seebeck coefficient for various carrier concentrations.²⁴ In Figure 11 a comparison is drawn between "single crystal" and small grain size material. It is evident that the thermoelectric figure of merit of highly disordered lead telluride type material with a mean grain size of $\sim 1\mu\text{m}$ is about 10 percent higher than equivalent "single crystal" or large grain size material.

3. Alloys based upon lead telluride

(i) Introduction

A realistic theoretical model for lead telluride, which included a multivallied structure, intervalley and intravalley scattering, non parabolic energy bands, acoustic phonon and optical phonon scattering; has been developed and close agreement obtained between theoretical and measured transport properties. This model was then employed in identifying alloys based upon lead telluride with the highest potential for improvement in their figure of merit as a result of phonon-grain boundary scattering. PbSnTe and PbGeTe are particularly favoured because large differences in atomic masses of the constituent atoms give rise to substantial alloy disorder scattering and these materials were investigated.

(ii) Reduction in the lattice thermal conductivity of PbSnTe and PbGeTe.

The results of calculating the ratio $\lambda_L(\text{sintered})/\lambda_L(\text{single crystal})$ as a function of grain size L , conveniently expressed in terms of a parameter D where $D = CT$ and T is the absolute temperature for PbSnTe and PbGeTe are displayed in figures 12 and 13.

Figure 12. χ , the ratio $\lambda_L(\text{sintered})/\lambda_L(\text{single crystal})$, plotted as a function of the parameter D and grain size L for PbTe-SnTe at 300K. Curve I, B=0 (undoped); curve II, B=0.01 (optimally doped).

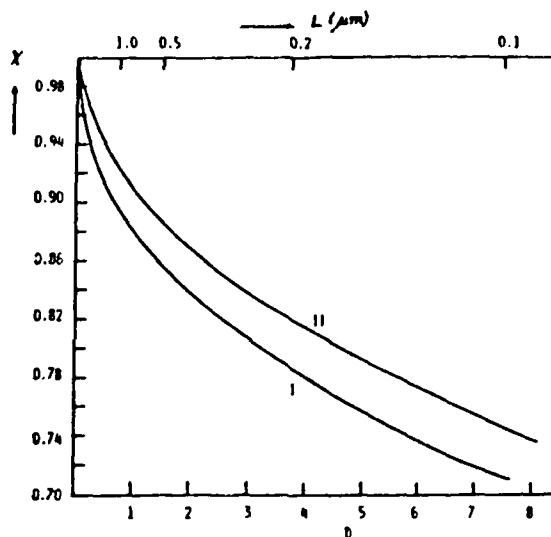
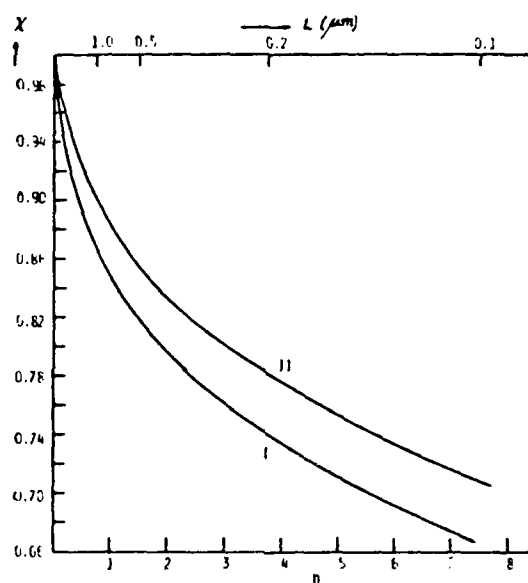


Figure 13. χ , the ratio $\lambda_L(\text{sintered})/\lambda_L(\text{single crystal})$, plotted as a function of the parameter D and grain size L for PbTe-GeTe at 300K. Curve I, B=0 (undoped); curve II, B=0.01 (optimally doped).



The basic characteristics of the PbTe system has been retained in the calculation and the effect of alloying with SnTe and GeTe is to produce disorder which can effectively scatter the high frequency phonons. This has the effect of enhancing the effectiveness of phonon-grain boundary scattering. Although there is some difficulty in making accurate predictions of the dependence of the lattice thermal conductivity on the various parameters because of a lack of experimental data and an uncertainty in fixing an appropriate value of k_0 it is possible to estimate the range over which the results will vary.

It is concluded that in undoped PbSnTe and PbGeTe ($B=0$) with a mean grain size of $0.5\mu\text{m}$ at 300K the percentage reductions in lattice thermal conductivity given by $[1 - \lambda_L(\text{sintered})/\lambda_L(\text{single crystal})] \times 100$ are 15 percent and 18 percent respectively. In optimally doped material (assuming carrier concentration to be similar to that of unalloyed lead

telluride the reductions are 11 percent and 14 percent respectively. A further reduction in mean grain size to $0.25\mu\text{m}$ would decrease the lattice thermal conductivity of lead telluride by 17 percent and PbGeTe by 21 percent. This is approaching the limit of the beneficial effect of a reduction in grain size as in this region electron grain boundary scattering becomes significant and leads to an undesirable decrease in the electrical conductivity.

VI EXPERIMENTAL PROGRAMME OF WORK.

1. Introduction

The theoretical model outlined in Section I provided a guide on the reduction in lattice thermal conductivity with decrease in grain size. The objective of the experimental programme of work was to substantiate the theoretical predictions and towards this end it was decided to attempt to prepare compacted material with a mean grain size of $<5\mu\text{m}$ and $<0.5\mu\text{m}$.

2. Charge material preparation

(i) $<5\mu\text{m}$ grain size

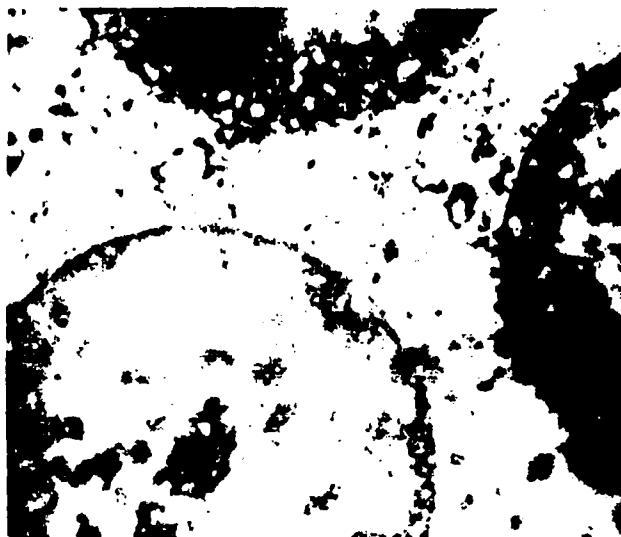
The starting material used in the investigation was a pulled, large grain size (up to 0.5cms) ingot of 2N-lead telluride supplied by Global Thermoelectrics*. 2N is a 3M* designation for lead telluride to which approximately 0.03 molecular percent PbI_2 has been added to increase the carrier concentration. The ingot was crushed under methanol in an agate pestle then ground wet for one hour in a two ball vibromill. The powder was sieved through a $5\mu\text{m}$ British Standard microsieve using methanol as a vehicle and assisted by ultrasonic vibrations.

(ii) $<0.5\mu\text{m}$ grain size

Decreasing the grain size of the charge material by an order of magnitude prescribed handling problems. Submicron size particles are airborne at low velocity draughts and all handling stages of the powder were carried out when wet with methanol. The $<5\mu\text{m}$ grain size sieved fraction obtained as described above was ground in an agate ball mill for one hour using methanol as a vehicle. A photomicrograph of the resultant powder dispersed in NONIDET P42 and viewed in transmitted light is shown in Figure 14. The powder rests on the base of a $5\mu\text{m}$ aperture microplate

* Global Thermoelectric Power Systems Ltd
PO Box 400
Bassano
Alberta, Canada

Figure 14. Photomicrograph of $<0.5\mu\text{m}$ lead telluride powder dispersed in NONIDET P42; $5\mu\text{m}$ microsieve aperture shown as a size comparison.



sieve and the operative provides a convenient size comparison for the particles. Considerable difficulty was encountered in satisfactorily dispersing these very small particles even when assisted by ultrasonic vibrations as is evident from the agglomerated appearance. No attempt was made to measure the size of the particles, but evidently the vast majority of particles are less than $0.5\mu\text{m}$. The charge is introduced into the die as a "slurry" and the methanol evaporated off insitu.

3. Hot Press

It is reported in the literature²⁷ that lead telluride can be successfully compacted using hot or cold pressing techniques. However, lead telluride is known to possess a relatively high vapour pressure and losses of constituents result in a change in transport properties; consequently initial attempts were made to cold compact the powders. The arrangement employed in this present study is shown in Figure 15. A cold compaction pressure of 300 MPa is recommended, consequently emphasis was placed on strength and stability with the die and supporting column machined in a number of interlocking sections. Provision for rapidly heating the die is made by locating the die inside a relatively large graphite cylinder. The die and plungers are fabricated from TZM alloy and machined to a press fit. The inside surface of the die is painted with liquid graphite and the faces of the plungers separated by high density graphite spacers.

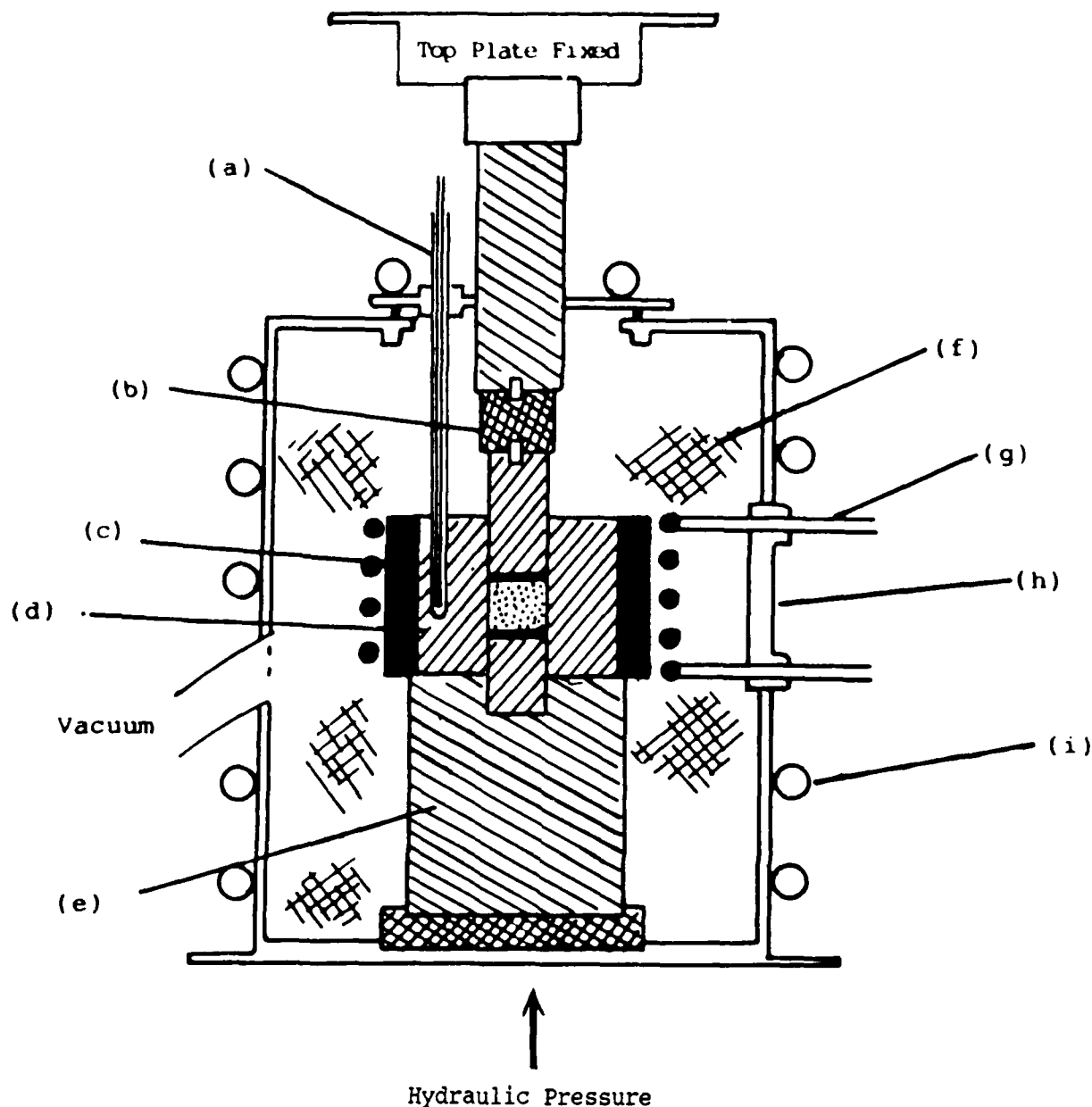


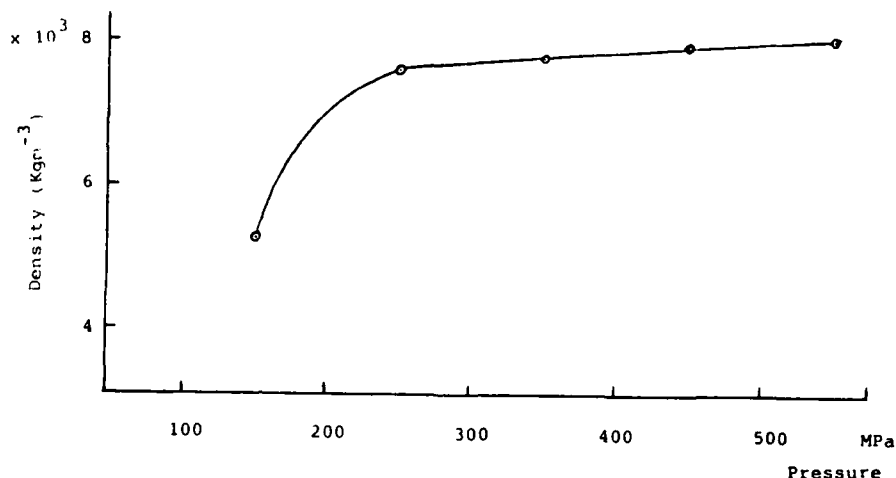
Figure 15.
Hot Press Arrangement

- | | |
|------------------------------------|------------------------------------|
| (a) Pt/Pt-Rd shielded thermocouple | (b) Silver steel packing block |
| (c) Graphite susceptor | (d) T2M die |
| (e) Mild steel support | (f) Silica wool thermal insulation |
| (g) r.f. induction coil | (h) PTFE insulator |
| (i) Water cooling | |

4. Pressing procedure

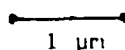
A series of cold compactions were carried out on $<5\mu\text{m}$ powder over a wide range of pressures. Single crystal density is 8.25 gm cm^{-3} and the density of the compacts increased with pressing pressure from 5.0 gm cm^{-3} at 150 MPa to 7.80 gm cm^{-3} at 400 MPa as shown in Figure 16. Although it should be noted that this graph is only a guide as its shape is strongly dependent upon the state of the particle surface and particle size.

Figure 16. Dependence of density of PbTe compacts with pressing pressure.



Cracks develop in compacts pressed at $>300\text{MPa}$ and they invariably break into sheet-like pieces in planes perpendicular to the pressing direction. The application of heat greatly reduces the required compaction pressure. Mechanically strong compacts with a grain size of $<0.5\mu\text{m}$ and densities of around 8.1 gm cm^{-3} were prepared by hot pressure sintering for 10 minutes at a pressure of approximately 100 MPa and a temperature of 1100K. Compacts of similar densities were also prepared with a grain size of $<0.5\mu\text{m}$, although these compacts were not as mechanically strong. As the main objective of this stage of the research programme was to determine the change in thermal properties with grain size rather than evaluate the effect of high temperature compaction on the electrical properties of PbTe subsequent physical characterisation and measurement of transport properties were made on hot pressed, high density compacts.

Figure 17. Photomicrograph of $<0.5\mu\text{m}$ grain size compacted lead telluride.



5. Physical Properties

The surface of the high density, pressed discs, after polishing down to $1/12\mu\text{m}$ size is smooth and void free when examined by optical microscopy. The grain structure of the compact is revealed by heating in an iodine etch at 368K for 5 minutes ($10\text{H}_2\text{O}$, 5gm NaOH and 0.2gm I_2)²⁸. A photomicrograph of $<0.5\mu\text{m}$ grain size compacted material is shown in Figure 14. It is apparent that the "larger grains" are agglomerates and that little, if any, grain growth has taken place. Density of the compacts were determined by the method of hydrostatic weighing. Error in density determination is less than 0.5 percent.

6. Transport Properties.

(i) Introduction

The transport properties, and in particular the electrical properties are determined by the stoichiometric ratio of its components. An excess of lead induces n-type electrical behaviour and an excess of tellurium, p-type by behaviour, carrier concentration of about $3 \times 10^{23}\text{m}^{-3}$ can be induced in this way. In thermoelectric application carrier densities an order of magnitude larger are required than those which can be achieved by changing the stoichiometric ratio. These higher values of carrier concentration are obtained by introducing foreign molecular species such as PbI_2 (electrons) and Na (holes). The solid solubility limit of the components are temperature dependent and is determined by the annealing temperature. The carrier concentration also depends upon the rate of quenching with more carriers remaining in solution if the material is rapidly quenched.

(ii) Seebeck coefficient and electrical resistivity measurements.

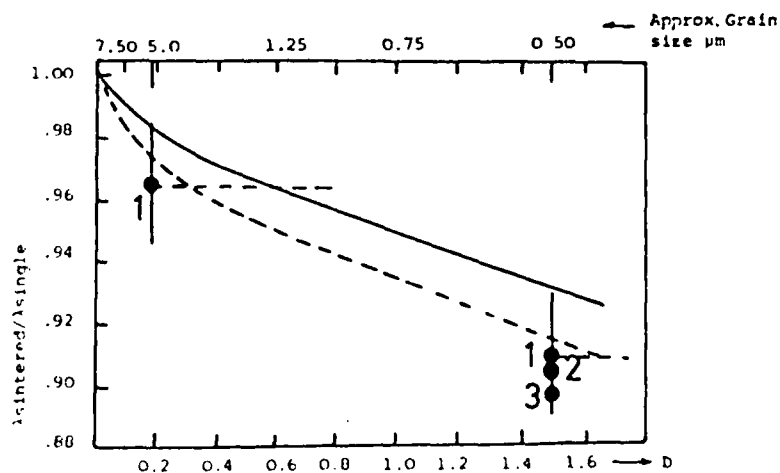
Seebeck coefficient measurements were made using a hot probe; accuracy of measurement is ± 3 percent. Electrical resistivity measurements were made using the four probe method; accuracy ± 2 percent. Measurements of Seebeck coefficient and electrical resistivity were made on the pressed compacts and compared with values obtained from measurements on discs having identical geometry and cut from the original "single crystal" ingot. The Seebeck coefficient and electrical conductivity of "as compacted" material differs considerably from that of single crystal. High temperature annealing is an established procedure for stabilizing the transport properties of semiconductors and the compacted materials have been subjected to a variety of annealing sequences. The effect of rapidly cooling the sample (quenching in water) is to "freeze in" the large number of carriers present at the higher

temperature and hence reduce the Seebeck coefficient. Rapid cooling, however, is accompanied by an increase in the strain energy of the sample, and results in a decrease in the carrier mobility and consequent increase in resistivity. To date electrical properties closest to single crystal have been obtained by annealing the compact in an argon atmosphere at 1040K for 3 hours followed by 4 hours at 700K and slowly cooling to room temperature. Seebeck coefficients very close to that of single crystal have been obtained whilst the electrical conductivity, although substantially reduced, remains significantly higher than single crystal value.

(iii) Thermal diffusivity and thermal conductivity measurements.

Room temperature thermal diffusivity measurements were made on hot pressed samples using a laser flash technique²⁹. Discs 5mm in diameter were cut from the $<5\mu\text{m}$ compacted material using an ultrasonic drill. Thermocouple contacts to the rear of the sample are made using pressure contacts. Optimum sample thickness for thermal diffusivity measurements was about 1mm, but samples of this thickness were too fragile and invariably fractured when subjected to the contacting pressure which was necessary to provide low electrical resistance contacts. Consequently samples 2mm thick were employed. As indicated previously compacts of $<0.5\mu\text{m}$ grain size material were relatively weak and proved difficult to machine. Thermal conductivity measurements were made on the polished

Figure 18. The reduction in thermal conductivity of PbTe with decrease in grain size (L) - optimally doped..... undoped (theoretical curves) ● Experimental values.



surface of these very small grain size samples. A suitable disc thickness is 1cm. A thermal comparator method was employed and again a comparison made between the compacted sample and one of identical geometry

cut from the "single crystal" ingot. The reduction in thermal conductivity with decrease in grain size (at room temperature) is shown in Figure 15.

vii Discussion and conclusion

All principle objectives of the programme of research have been achieved. A semiquantitative theoretical model of lead telluride has been used to estimate the relative reduction in lattice thermal conductivity, compared to that of single crystal, which accompanies the use of small grain size material. It was predicted that in material with a mean grain size of $1\mu\text{m}$, the reduction would be around 5 percent. A procedure has been developed for comminuting very small grain size material and a number of high density compacts of lead telluride successfully prepared. Measurements on small grain size compacts substantiated the predicted reduction in thermal conductivity with decrease in grain size.

A realistic theoretical model has been developed for lead telluride. Very good agreement was obtained between the theoretical values of the thermal conductivity and experimental values cited in the literature. The thermoelectric figure of merit is optimised at a carrier concentration of about $2 \times 10^{24} \text{m}^{-3}$. Provided the electrical properties can be maintained close to "single crystal" value the thermoelectric figure of merit in highly disordered alloys of lead telluride with a mean grain size of $\sim 1\mu\text{m}$ and optimum doping is calculated to be about 10 percent higher than equivalent single crystal values.

The model has been used to explore the thermal properties of alloys based upon lead telluride. PbSnTe and PbGeTe hold out the best potential for improvement in the figure of merit, as a result of a decrease in the lattice thermal conductivity due to phonon-grain boundary scattering. At room temperature the lattice thermal conductivity of PbSnTe and PbGeTe , optimally doped and with a grain size of $0.25\mu\text{m}$, would be reduced by 17 percent and 21 percent respectively.

Although not strictly part of this current research contract, the behaviour of the electrical transport properties of fine grained compacts is very relevant to any attempt to improve the thermoelectric figure of merit. The results of a limited programme of work in this area indicate that Seebeck coefficients very close to single crystal values can be obtained by annealing the fine grain compacted material. Electrical resistivity values can also be substantially reduced although values remain significantly higher than equivalent single crystal values. A systematic investigation is required to establish the annealing procedure

which optimises the electrical properties of these compacts.

It is concluded that the thermal conductivity of lead telluride type material can be substantially reduced and hence the thermoelectric figure of merit significantly improved through the use of very small grain size material, provided the electrical properties can be maintained at values close to those of equivalent single crystal material. As annealing procedures are routinely employed in controlling the electrical properties of established thermoelectric materials it is not anticipated that the development of a suitable annealing procedure for very fine grained lead telluride type material would present great difficulties.

VIII ACKNOWLEDGMENTS

Dr C M Bhandari is thanked for his contribution to this project and the United States Army, under Contract No. DAJA 45-84-C-0029, is acknowledged for supporting this work and Dr Bhandari's Visiting Research Fellowship. Global Thermoelectrics is acknowledged for providing the lead telluride material and Mrs Kathleen Edwards of the Department of Physics, Electronics and Electrical Engineering, UWIST, is thanked for typing the manuscript.

IX REFERENCES

1. G Guazzoni and W Swaylik, Proceedings of the 4th International Conference on Thermoelectric Energy Conversion, University of Texas at Arlington 1982, p1.
2. G McLane and G Guazzoni, Proceedings of the 5th International Conference of Thermoelectric Engergy Conversion, University of Texas at Arlington 1984, p18.
3. A F Ioffe, Semiconductor Thermoelements and Thermoelectric Cooling, Infosearch, London 1957.
4. Thermoelectric Materials and Devices, edited by I B Cadoff and E Miller (Reinhold, New York, 1959).
5. P J Bateman, Contemp.Phys.2. 302 (1960).
6. H J Goldsmid, Applications of Thermoelectricity (Methuen, London 1960).
7. Thermoelectricity; Science and Engineering, edited by R W Ure Jr. and R R Heikes (Interscience, London 1961).
8. F D Rosi, Solid State Electron. 11 833 (1968).
9. D A Wright. Metall. Rev. 15. 147 (1970).
10. D M Rowe. Proc.IEE 125 (11R), 1113 (1978).
11. D M Rowe, Proc of 4th International Conference on Thermoelectric Energy Conversion, University of Texas at Arlington, 10th-12th March (1982), p96.
12. D M Rowe. PhD Thesis, Unversity of Wales.
13. H J Goldsmid and A Penn. Phys. Lett. 27A 523 (1968).
14. J E Parrott, J Phys. C 2, 147 (1969).
15. C M Bhandari and D M Rowe Contemp Phys Vol 21, No.3 219 (1980).
16. H R Meddins and J E Parrott. J Phys. C 9, 1263 (1976).
17. C M Bhandari and D M Rowe. J Phys. C 11, 1787 (1978).
18. W Zawadzki Adv.Phys.23, 437, (1974).
19. I Yu Ravich, B A Efimova, I A Smirnov, Semiconducting Lead Chalcogenides (Plenum, New York) 1970.
20. I Yu Ravich, B A Efimova, V I Tamarchenko, Phys.Status Solidi B.43. 11 (1971).
21. C Herring. Bell System. Tech.J. 34, 237 (1955).
22. D M Rowe and C M Bhandari, Modern Thermoelectrics, Holt Reinhart and Winston, London (1983).

23. D A Wright Metall.Rev. 15, 147 (1970).
24. B A Efimova, L A Koldmoets, I Yu Rovich, T S Stavitskoya; Soviet Physics - Semiconductors 4, 1653 (1971).
25. C M Bhandari and D M Rowe: J Phys D 16. L75 (1983).
26. N K S Gaur, C M Bhandari and G S Verma. Phys Rev 144 628 (1966).
27. Electronics Materials Review No.7, Thermoelectric materials Noyes Data Corporation, New Jersey (1970).
28. P J Holmes (Editor) The Electrochemistry of Semiconductors. Academic Press, London and New York p 375 (1962).
29. D M Rowe and V S Shukla, J.Appl Phys 52 11, 7421 (1981).

Erratta Detected After Publication

by $D=CT$ where T is the temperature. $A=0$ corresponds to unalloyed material with no disorder present, $B=0$ corresponds to undoped material and $C=0$ to single crystal material. In general $\lambda(A,B,C=0) = \lambda_{\text{single}}$ represents the lattice thermal conductivity of a doped single crystal alloy while $\lambda(A,B,C) = \lambda_{\text{sintered}}$ represents the lattice thermal conductivity of a compacted (sintered) alloy.

3. Electronic contribution to the thermal conductivity

(i) Introduction

Lead telluride and its alloys possess a narrow energy band gap (E_g). These materials have small electron effective masses and the density of states which varies as $m^{3/2}$ is also relatively small. Consequently a relatively small number of carriers will be sufficient to fill the bands up to high energy levels. The effective mass of electrons near the top of the conduction band become energy dependent¹⁶. In the model adopted a two band conduction band is considered with the following main features; the band extrema for the conduction and valence bands are assumed to be located at the same k value. The energy separation from the other bands at this k value is greater than the main energy gap and the momentum operator has non-zero matrix elements between the states corresponding to the extremal points. Non-parabolicity and the effective mass of both bands are defined by the interaction of the electron and hole bands only. The energy dispersion law is of the form:-

$$\frac{\hbar^2 k_{\perp}^2}{2m_{\perp 0}^*} + \frac{\hbar^2 k_{\parallel}^2}{2m_{\parallel 0}^*} = E \left(1 + \frac{E}{E_g} \right)$$

are.
 k_{\perp} and k_{\parallel} are the transverse and longitudinal components of the wave vector and $m_{\perp 0}^*$ and $m_{\parallel 0}^*$ are the components of the effective mass tensor near the band extremum. This is usually referred to as the "Kane model". The energy dependence of the effective mass is given by :-

$$m^* = m_0^* \left[1 + \frac{2E}{E_g} \right]$$

$$\text{where } L_n(A, B, C) = \int_0^1 \frac{x^n dx}{Ax^4 + x^2 + Bx + C}$$

here $x = \hbar\omega/k_B T$ and $k_0 = \tau_U/\tau_N$ is the ratio of the phonon relaxation times for Umklapp and Normal processes, k_B is Boltzmann's constant and T is the temperature. There is no advantage in this present study to undertake detailed calculations of the contributions to the thermal conductivity from separate polarizations and an average acoustic branch is assumed. The various phonon relaxation times are as described in the literature;¹⁴⁻¹⁶⁻¹⁷ the phonon-electron scattering relaxation time is given by

$$\tau_{pe}^{-1} = B'x$$

A, B and C are given by

$$A = \frac{\pi^2 \Omega_0 \lambda_0 \omega_D}{2 V_S^2 k_B \left(1 + \frac{5k_0}{9}\right)} \quad \begin{array}{l} \text{Alloy disorder} \\ \text{scattering} \end{array}$$

$$B = \frac{2\pi^2 \lambda_0 \hbar B'}{k_B L \omega_D^3 \left(1 + \frac{5k_0}{9}\right)} \quad \begin{array}{l} \text{Free carrier} \\ \text{scattering} \end{array}$$

$$C = \frac{2\pi^2 \lambda_0 \hbar^2 V_S^2}{k_B L \omega_D^3 \left(1 + \frac{5k_0}{9}\right)} \quad \begin{array}{l} \text{Grain boundary} \\ \text{scattering} \end{array}$$

delete

The various parameters have the same meaning as in the literature¹⁴⁻¹⁶⁻¹⁷. It is usual to express C in terms of a parameter D, which is inversely proportional to the grain size L and they are related

The appropriate expression for $\tau(\eta)$ which includes the energy dependence of M is given by^{19,20}

$$\tau(\eta)^{-1} = \frac{\hbar k_B T (\rho/N_V)}{\hbar C_1} \epsilon^2 \left[1 - \frac{8B_g \eta (1+B_g \eta)}{3(1+2B_g \eta)^2} \right]$$

where C_1 is the elastic constant related to the average sound velocity, (ρ/N_V) is the density of state in a given valley and ϵ is the deformation potential constant.

The Lorenz factor is given by:-

$$r = \left[\frac{L_{-2}^1}{L_{-2}^0} \right] - s^2$$

where $s = L_{-2}^1 / L_{-2}^0$, and $n_{L_g^m}$ are generalised.

Fermi integrals are defined as:-

$$n_{L_g^m}(\xi) = \int_0^\infty \left[- \frac{\partial f}{\partial \eta} n^n [\eta(1+B_g \eta)]^m (1+2B_g \eta)^2 d\eta \right] \quad \text{--- } d\eta$$

The reduced electrical conductivity is given by:-

$$\sigma' = k N_V L_{-2}^0 \frac{T}{(m_C^* \lambda_L)}$$

With the carrier concentration n related to the reduced Fermi energy ξ , by the expression:-

$$n = \frac{(2m_{d_o}^* k_B T)^{3/2}}{3\pi^2 \hbar^3} O_{L_o}^{3/2}$$

The carrier mobility μ_{ac} due to acoustic phonon scattering is given by:-

$$\mu_{ac} = \frac{\text{constant}}{m_{C_o}^* m_{d_o}^{3/2} T^{3/2}} \frac{O_{L_{-2}}'}{O_{L_o}^{3/2}}$$

3.(iii) Carrier scattering by polar optical phonons

The carrier relaxation time for scattering by polar optical phonons is given by²⁰

$$\tau_{op}^{-1} = \frac{2^{1/2} e^2 k_B T m_d^{*1/2}}{h^2 (\eta k_B T)^{1/2}} (\epsilon_\infty^{-1} - \epsilon_0^{-1}) \frac{1+2\beta_g \eta}{(1+\beta_g \eta)^{1/2}}$$

$$\times \left[[1 - \epsilon_\infty \eta n(1 + \epsilon_\infty^{-1})] - \frac{2\beta_g \eta (1 + \beta_g \eta)}{(1 + 2\beta_g \eta)^2} [1 + 2\epsilon_\infty + 2\epsilon_\infty^2 - \eta n(1 + \epsilon_\infty^{-1})] \right]$$

The Lorenz factor is given by :-

$$r = [^2L_{-2}^2 / ^0L_{-2}^2] - \delta^2$$

$$\text{where } \delta = ^1L_{-2}^2 / ^0L_{-2}^2$$

In the calculations, screening effects have not been taken into account. Polar optical scattering although appreciable in lead telluride materials, is not the dominant scattering mechanism. Consequently neglecting screening effects will not substantially affect the overall electronic transport properties.

The reduced electrical conductivity can be expressed as:-

$$\sigma' = N_V K' T^2 f(\theta_0/T) m_d^* {}^0L_{-2}^2 / (\lambda_L m_C^*)$$

$$\text{with } K' = \frac{4k_B^2}{3e^2 \pi^2 \hbar (\epsilon_\infty^{-1} - \epsilon_0^{-1})}$$

where ϵ_0 and ϵ_∞ are the static dielectric constant and the dielectric constant at high frequencies respectively. θ_0 is the temperature which corresponds to the optical phonon frequency at the zone boundary.

The carrier mobility μ_{op} due to optical phonon scattering is given by:-

$$\mu_{op} = \frac{K'' f(\theta_0/T) {}^0L_{-2}^2}{T^{1/2} m_d^* m_C^* {}^0L_0^{3/2}}$$

$$\text{where } K'' = \frac{8\hbar^2 (2\pi k_B)}{3E (2\pi k_B)^{3/2} (\epsilon_\infty^{-1} - \epsilon_0^{-1})}$$

END

DTIC

6-86